Paper:

Alkhudhiri, A. & Hilal, N. (2016). Air Gap Membrane Distillation: A detailed study of high saline solution. *Desalination*

http://dx.doi.org/10.1016/j.desal.2016.07.046

Air Gap Membrane Distillation: A detailed study of high saline solution

Abdullah Alkhudhiri[a], Nidal Hilal[b]

[a] King Abdulaziz City for Science and Technology (KACST), Nanotechnology Centre, Riyadh, Saudi Arabia

[b] Centre for Water Advanced Technologies and Environmental Research (CWATER), College of Engineering, Swansea University, United Kingdom

Abstract

An experimental study is used to examine the effect of high concentration of several salts, i.e., NaCl, $MgCl_2$, Na_2CO_3 and Na_2SO_4 on permeate flux and rejection factor by air gap membrane distillation (AGMD). A comparative study involving three different membrane pore sizes (0.2, 0.45 and 1.0 μm) were performed to investigate the influence of pore size on energy consumption, permeate flux and rejection factor. The permeate flux decline is higher than that predicted from the vapour pressure reduction. Furthermore, the energy consumption was monitored at different membrane pore size and was found to be increased when the concentration increased.

Key words: Air gap membrane distillation (AGMD); High saline solution; Desalination ; Water treatment

1. Introduction

Salinity is one of the most pressing environmental economic problems in arid countries. Desalting systems have long proven effective in the arid countries, such as in the Arabian Gulf. Water desalination can be performed using different techniques, such as thermal and membrane processes. Membrane distillation (MD) have the benefits of thermal and membrane technologies, as it is considered a thermally-driven separation process. Vapour molecules are only able to pass through a porous hydrophobic membrane. As a result, high purity water will be obtained from aqueous solution [1-4]. This separation process is driven by the vapour pressure difference existing between the porous hydrophobic membrane surfaces. Consequently, MD processes have vapour pressure difference as the driving force. Permeate flux, in general increases linearly with trans-membrane vapour pressure [2-7].

There have been many studies to explore the impact of high salt concentration on the membrane permeability. The influence of high salt concentration and complex solution such as produced water on the permeate flux and rejection factor was reported [8-11]. Yun et al [10] found that, there was a noticeable variation on membrane permeability with time. As a result, it is hard to determine the permeate flux by using the existing models. They assumed that, the properties of the boundary layer solution (at the membrane surface) reaches the saturation and varies from the bulk solution. Indeed, the solution features are changed; for example, the density and viscosity increase, while the vapour pressure decreases [8, 10-12]. Moreover, the boiling point and surface tension rise when the concentration increases [12-15].

In addition, Li et al. [16], indicated that the permeate flux reduction becomes significant as salt concentration exceeds 2.0 M. The permeate flux of KCl, NaCl and $MgCl_2$ solutions reduced by 44.4% , 59.6% and 86.8% as the salt concentration increased from 2.0 to 4.0 M. In addition, they pointed out that the impact of viscosity on the permeate flux could not be neglected at high salt concentration.

Moreover, Safavi and Mohammadi [9], employed VMD to treat highly saline solution. They concluded that, the permeate flux is better with decreasing the feed concentration. However, the rejection factor is not affected by the feed concentration.

Fouling is a deposition of unwanted materials such as scale, suspended solids and insoluble salts on the external surfaces of the membrane (Fig 1). Kullab and Martin [17] pointed out that fouling and scaling lead to blocking the membrane pores, which reduces the effective membrane, and therefore the permeate flux obviously decreases. These may also cause a pressure drop, and higher temperature polarization effect. Gryta [18] indicated that the deposits formed on the membrane surface leads to the adjacent pores being filled with feed solution (partial membrane wetting). Moreover, additional mass and heat resistance will be created by the fouling layer (Eq.1 and 2), which is deposited on the membrane surface. As a result, the overall heat and mass transfer coefficient of the membrane decreased. For DCMD, Gryta and Goh et al. [19, 20] specified:

$$J = \frac{P_f - P_{f,fouling}}{R_f} = \frac{P_{f,fouling} - P_{f,m}}{R_{fouling}} = \frac{P_{f,m} - P_{p,m,}}{R_m} = \frac{P_{p,m} - P_p}{R_p} \quad (1)$$

where $\frac{P_f - P_{f,fouling}}{R_f}$ represents the mass transfer through the feed boundary layer; $\frac{P_{f,fouling} - P_{f,m}}{R_{fouling}}$ represents the mass transfer through the fouling layer ; $\frac{P_{f,m} - P_{p,m,}}{R_m}$ represents mass transfer through the membrane ; $\frac{P_{p,m} - P_p}{R_p}$ represents mass transfer through the permeate.

R_f, $R_{fouling}$, R_m , R_p are the resistance in the feed boundary, fouling layer, membrane and permeate boundary respectively.

$$h_f(T_f - T_{f,foulig}) = \frac{k_{fouling}}{\delta_{fouling}}(T_{f,fouling} - T_{f,m}) = \frac{k_m}{\delta}(T_{f,m} - T_{p,m}) + J\Delta H_v$$

$$= h_p(T_{p,m} - T_p) \quad (2)$$

where $k_{fouling}, \delta_{fouling}$ *and* $T_{f,fouling}$ are the fouling layer thermal conductivity, thickness, and fouling layer temperature, respectively.

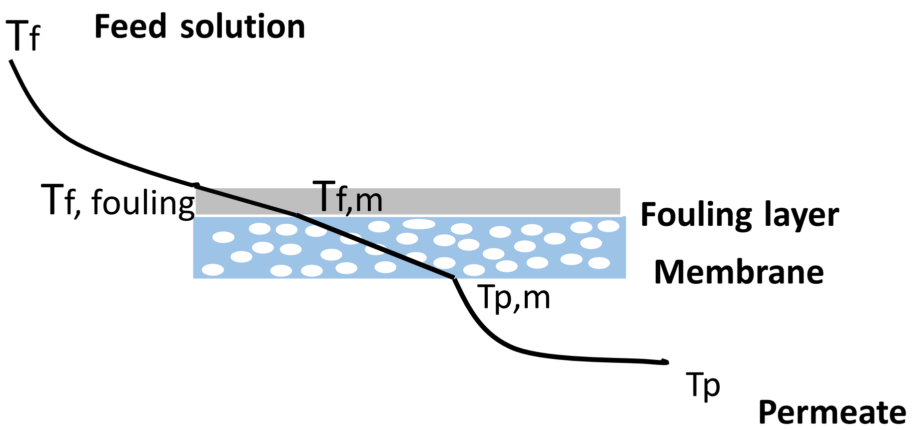

Fig.1. Temperature profile across fouled membrane

El-bourawi [21] proposed that scale formation and deposition at membrane surfaces may diminish the membrane hydrophobicity and cause water logging of some membrane pores. Tun et al. [22] examined the effect of high concentration of NaCl and Na_2SO_4 on the permeate flux. The flux gradually decreases during the MD process, until the feed concentration reaches the supersaturation point, and then the flux decreases sharply to zero. The membrane was completely covered by crystal deposits.

The influence of high concentrations on permeate flux, salt rejection factor, and energy consumption was examined in this work. In addition, the effect of pore size on the permeate flux and rejection factor was analysed too.

2. Experimental procedure and material

The influence of a wide range of concentrations of NaCl, $MgCl_2$, Na_2CO_3 and Na_2SO_4 on permeate flux, salt rejection factor, and energy consumption was examined as shown in table 1. In addition, the effect of pore size was investigated by three commercial membrane pore sizes (0.2, 0.45 and 1.0μm). The experimental tests were achieved by AGMD module, as shown in Fig.2. Three types of flat sheet polytetrafluoroethylene (PTFE) microporous hydrophobic membranes were used in this work. PTFE has excellent chemical resistance (nonreactive) being unaffected by almost all chemicals. Moreover, it is insoluble and thermally stable to high temperatures (up to 260 ^{o}C) [23] . These membranes, manufactured by Sterlitech corporation, were used to filter high saline solutions. The membrane cell was maintained in a horizontal position. The feed solution was maintained in direct contact with the membrane surface. Furthermore, the heat was supplied to the feed by a heating coil. The feed reservoir was insulated to minimize the heat losses. The feed temperature can be manipulated and controlled by an Autotune temperature controller. The feed flow rate was heated and maintained constant at 50°C and 1.5 l/min during the experimental run. Also, the cooling temperature can be selected and controlled at the desired level by a refrigerated thermostatic bath (LTD 6G) supplied by Grant Instruments, and then pumped at a constant flow rate (8.5 l/min) and constant temperature (10°C) to the bottom of the cell . In addition, the hot feed and cooling water are pumped in opposite flow directions in a closed system within the membrane cell. The inlet and outlet temperatures of the feed solution and the cooling water were continually measured using four (T-type) thermocouples placed at the inlets and outlets of the membrane cell. In order to measure accurate temperature for each thermocouple, these were calibrated.

The permeate flux (J) was measured by weighing the obtained permeate during a predetermined time using an electronic balance which connected to a computer:

$$J = \frac{W}{A\,\Delta t} \qquad (3)$$

Where W is the obtained permeate weight and A is the membrane area.

Furthermore, the concentration of single salt solution can be determined by measuring the conductivity. The electrical conductivity of the feed was monitored and recorded hourly by conductivity meter. However, the electrical conductivity of the permeate concentration was measured and recorded at the end of the experiment; the rejection factor can be calculated:

$$Reiection\ Factor = 1 - \frac{C_p}{C_{f,avg}} \times 100 \quad (4)$$

It is worthwhile stating that the energy consumption in each AGMD experiment was measured using the energy meter that registers the amount of electric energy consumed (in kWh), including all AGMD equipment, such as heating and cooling systems as well as the feed circulation pump.

Table 1: Range of concentration of single salts used in the filtration experiments.

Single Salt	NaCl	$MgCl_2$	Na_2SO_4	Na_2CO_3
Lowest concentration (ppm)	5844	4760	4260	5300
Highest Concentration (ppm)	180000	95210	142000	106000

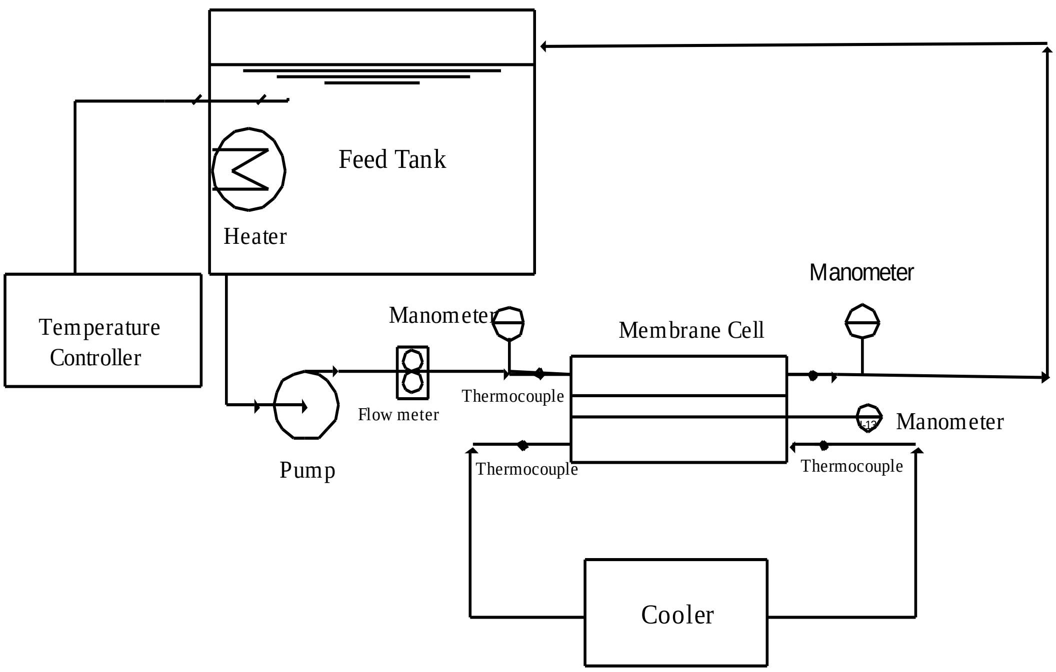

Fig. 2. Schematic diagram of the AGMD used in this work.

3. Result and discussion

3.1 Water activity and vapour pressure

Water activity of aqueous solution is the ratio between the vapor pressure of water in the solution to the vapor pressure of pure water at the same temperature. Water activity indicates to the total amount of pure water existing in the material. According to this definition, the value of unity for Water activity reveals to pure water, whereas zero reveals the total absence of water molecules.

For the ideal solution, the water activity is equal to the mole fraction of water in the solution [24]:

$$a_w = x_w = 1 - x_s \quad (5)$$

where x_s is mole fraction of solute.

However, the water activity for non-ideal solution can be evaluated by [24]:

$$a_w = (1 - x_s)\, exp(\,\alpha\, x_s^2 + \,\beta\, x_s^3) \quad (6)$$

Where α and β are parameters equal to 1.825 and -20.78 respectively for NaCl, and equal to 11.859 and -404.5 respectively for $MgCl_2$.

Table 2: The influence of concentration on the water activity

NaCl molar fraction	Water Activity (a_w) [25]
0	1
0.00179	0.9966
0.0035	0.9934
0.0053	0.99
0.016	0.97
0.0261	0.95
0.0356	0.93
0.044	0.91
0.0527	0.89

Na_2SO_4 molar fraction	Water Activity (a_w) [25]
0	1
0.0018	0.993
0.0089	0.98
0.0177	0.965
0.0263	0.948
0.0347	0.935
0.043	0.918

$MgCl_2$ molar fraction	Water Activity (a_w) [24]
0	1
0.0008	0.999207377
0.0009	0.999109303
0.0036	0.996534344
0.0072	0.993260559
0.01	0.990773888
0.014	0.987198142

In terms of the concentration impact on water activity, Martínez [8] and Sparrow [26] indicated that there was a considerable decrease in water activity as concentration increases. However, the influence of temperature on water activity is almost negligible [25].

The effect of both concentration and temperature on the vapour pressures for aqueous salt solution can be evaluated by considering the water activity at the feed and permeate sides, such that:

$$P(T, x) = P^{*}(T)\, a_w(x) \quad (7)$$

Where, $a_w(x)$ is water activity as a function of concentration, and $P^{*}(T)$ is vapour pressure of pure water at a given temperature, which can be calculated by Antoine equation:

$$P^{*} = Exp\left(23.238 - \frac{3841}{T-45}\right) \quad (8)$$

Figures 3-6 show the effect of concentration on vapour pressure.

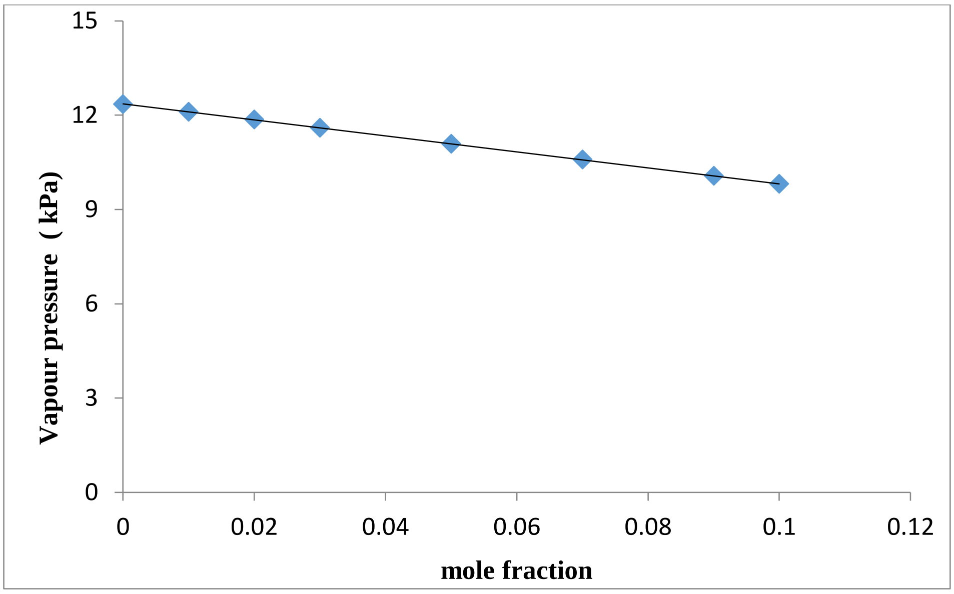

Fig. 3. Effect of concentration on the vapour pressure for NaCl

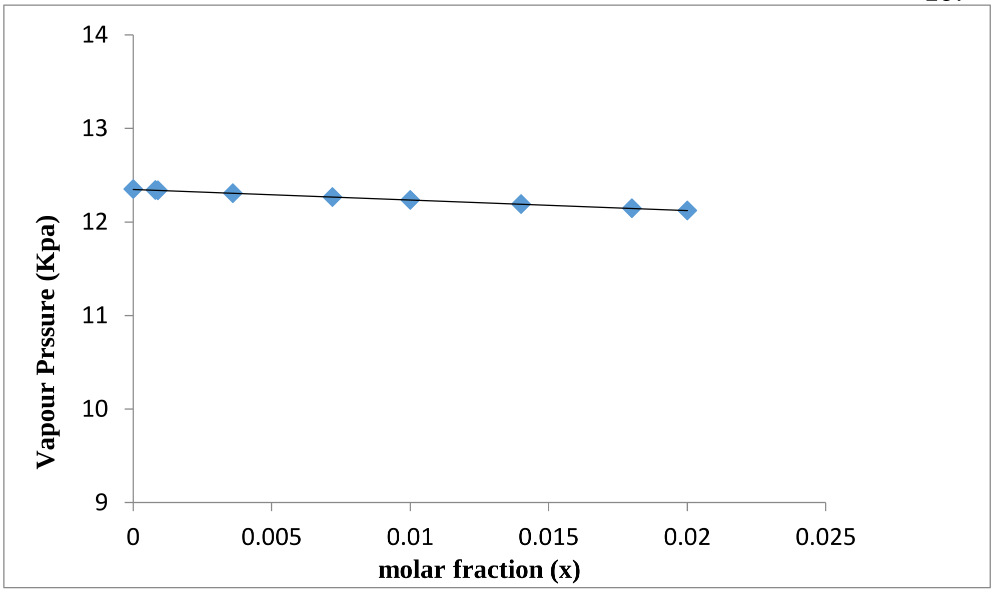

Fig. 4. Effect of concentration on vapour pressure for $MgCl_2$

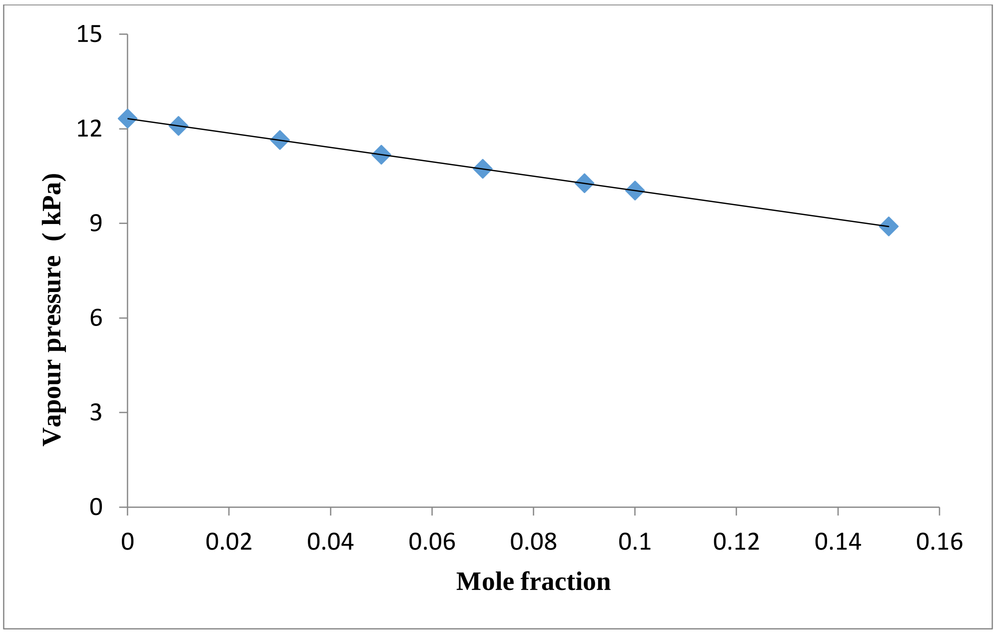

Fig. 5. Effect of concentration on vapour pressure for Na_2SO_4

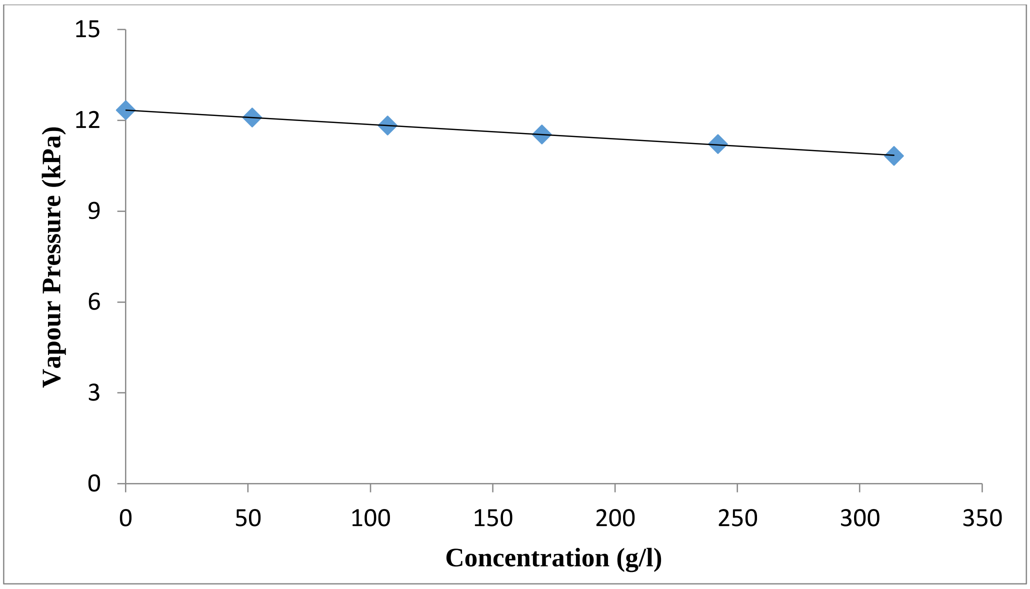

Fig. 6. Effect of concentration on vapour pressure for Na_2CO_3 [27]

3.2 The effect of Concentration and the pore size effect

It is obvious from the results that the permeate flux decreases when the concentration increases. It can be summarised that the vapour pressure plays an important role in permeate flux. This decrease can be referred to the water activity and vapour pressure reduction, and thereby reduced driving force (Fig 7 - 10). In addition, vapour pressure reduction means that less vaporization of water occurs at the membrane surface causing a decrease in amount of vapour flows through the membrane. Moreover, the solute is kept in by the membrane, then accumulates on the membrane surface. As a consequence, the feed concentration at the feed membrane surface will gradually increase, and then the temperature at the membrane surface is different (lower) than the bulk temperature measured in the feed. Furthermore, Qtaishat et al. [28] and Safavi and Mohammadi [9] stated that, in the case of aqueous solution, the salt will build an additional boundary layer adjacent to the membrane surface (concentration polarization). This boundary layer together with temperature boundary layer (temperature polarization) reduce the driving force. Moreover, Lawson and Alkhudhiri [29, 30] specified that , as a consequence of the raised of concentration polarization and temperature polarization effects, the mass and heat transfer coefficients at the boundry layer decreased. Moreover, Concentration polarization can cause a membrane wetting by scaling and building up of salt crystals on the membrane surface. Shirazi et al. [31] reported that, the particulate matters that are smaller than the membrane pore size will plug the membrane pores, in addition to the formation of cake on the membrane surface caused by accumulation of particles on the membrane surface.

It is worth stating that the permeate flux decay is higher than that predicted from the vapour pressure reduction. The explanation of this decrease is attributed to the fouling phenomenon, change in the solution layer feature facing the membrane surface, such as viscosity and to the temperature polarization phenomena. Similar results have also been reported by Drioli et al [7].

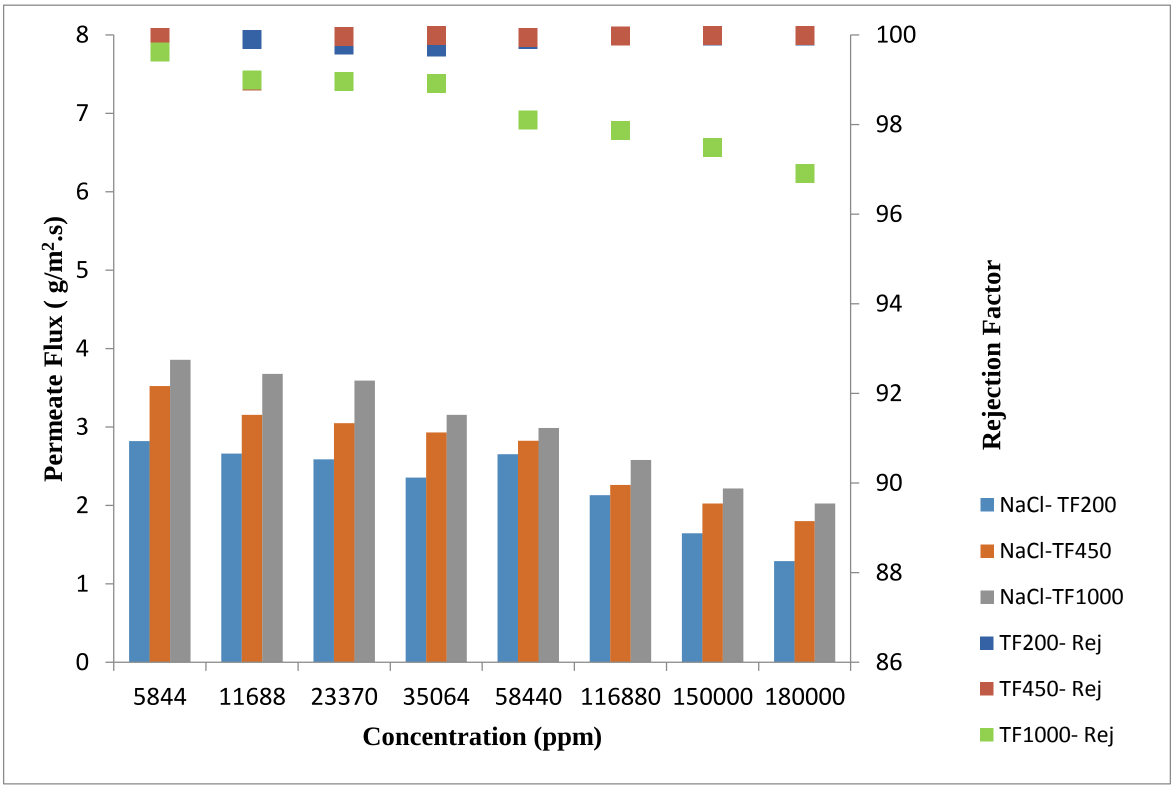

Fig. 7. The permeate flux and pore size effect for NaCl at different concentration

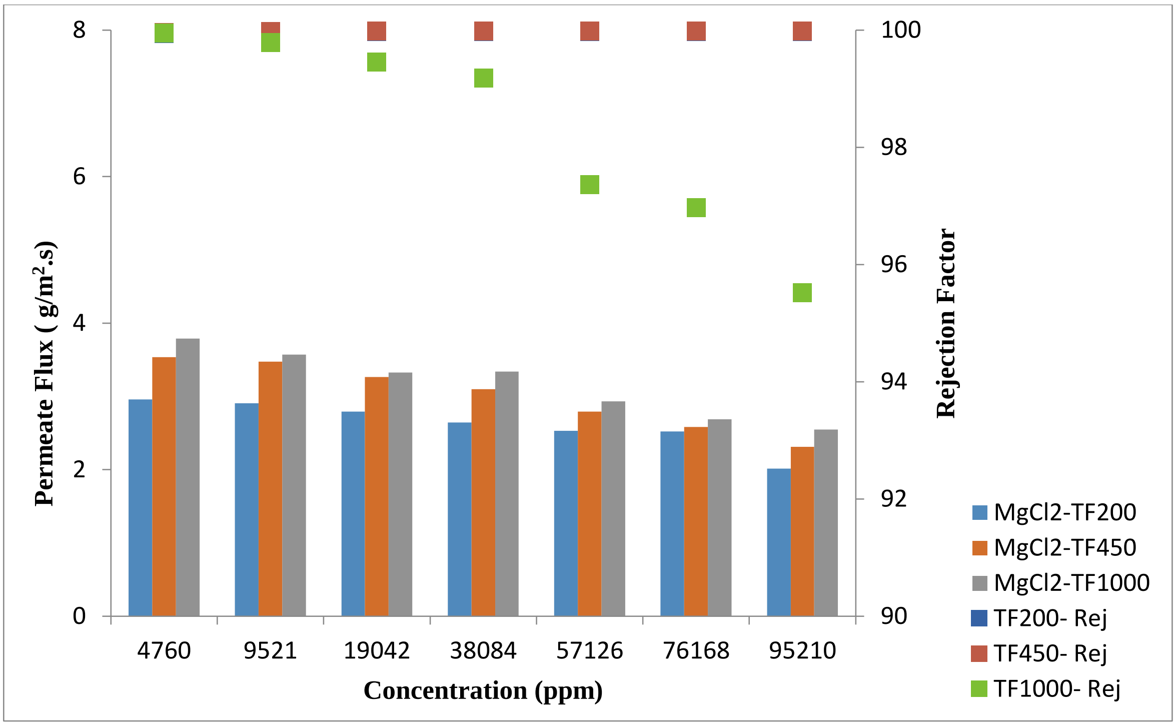

Fig. 8. The permeate flux and pore size effect for $MgCl_2$ at different concentrations

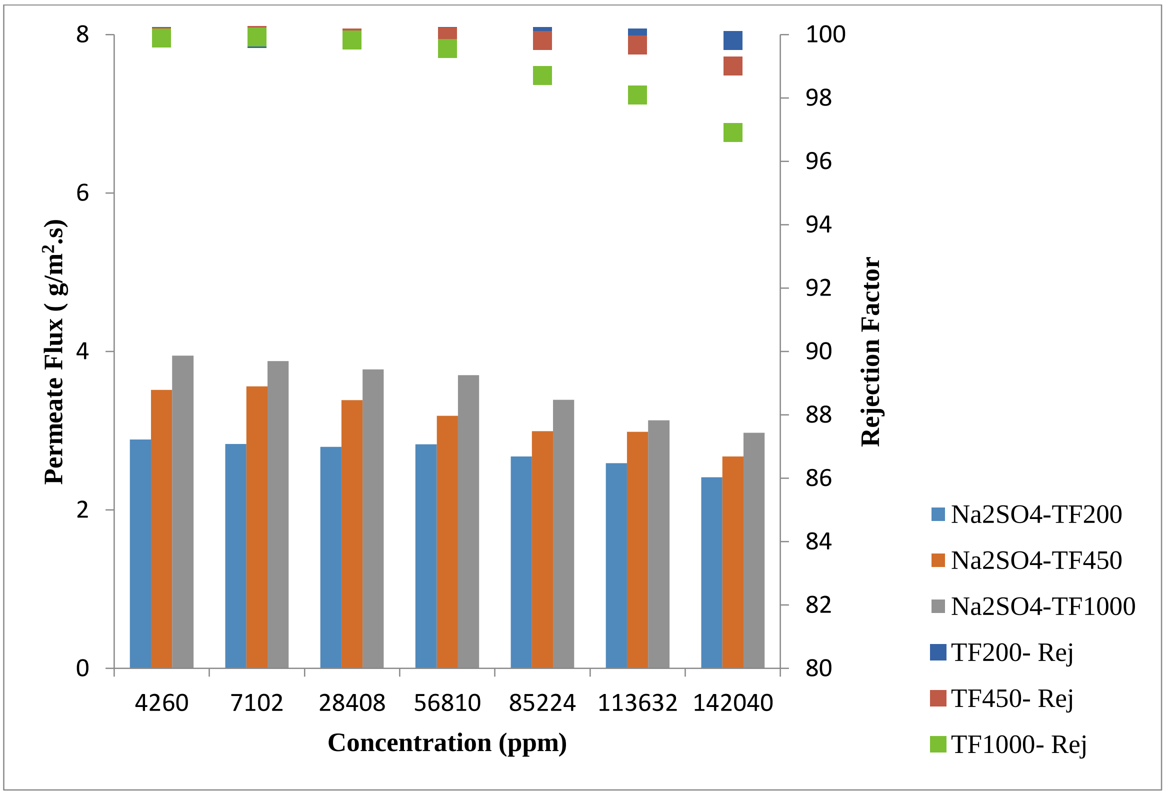

Fig. 9. The permeate flux and pore size effect for Na_2SO_4 at different concentrations

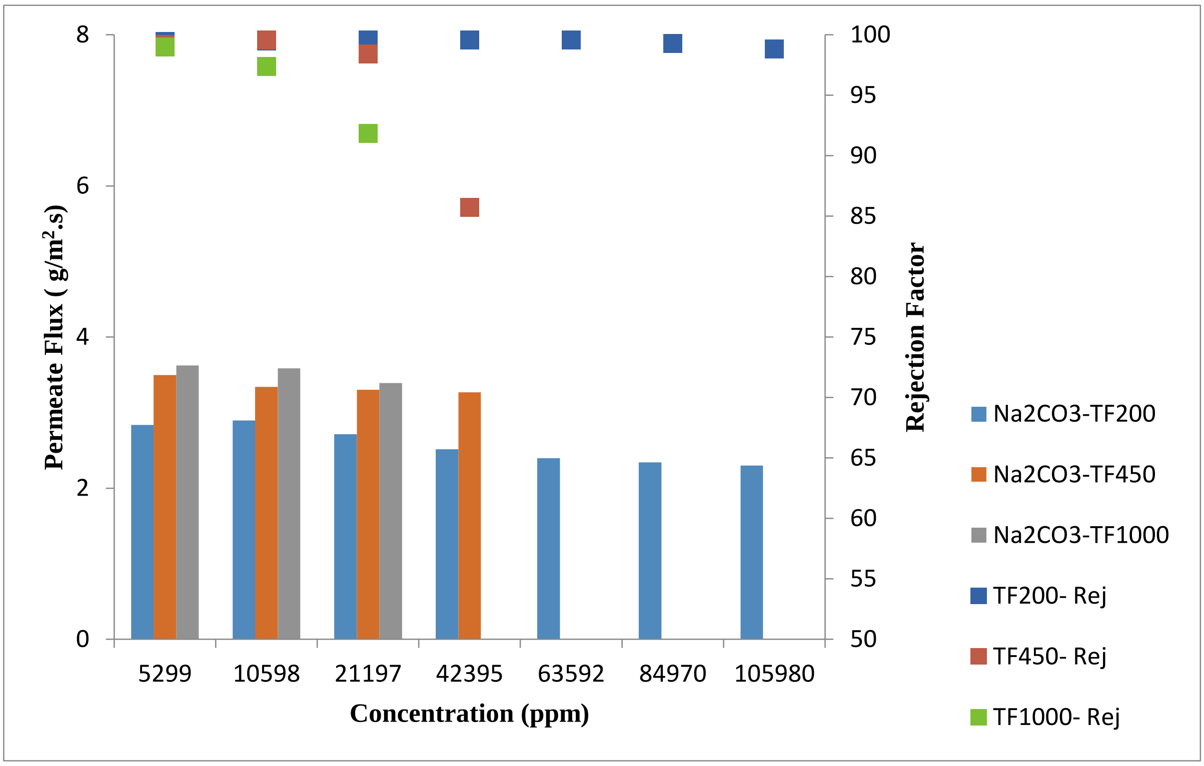

Fig. 10. The permeate flux and pore size effect for Na_2CO_3 at different concentrations

The effects of membrane pore size on permeate flux are shown in Figure 7-10 too. The permeation flux for NaCl at concentration 180,000 ppm increases from 1.289, 1.800 to 2.023 g/m^2.s in going from TF200, TF450 to TF1000 respectively. As shown in table 3, this corresponds to an enhancement of 39.6 % in the pure water flux corresponding to an increase in the mean pore size of 125% (from TF200 to TF450). The same enhancement of permeation flux is also noticed for the other saline solutions. This is a direct evidence of the enhanced mass transfer in the pores, which are subjected to Knudsen /ordinary diffusion mechanism [21].

Table 3: The influence of pore size on the permeate flux

Salt type and concentration	The percent increase from TF200 to TF450	The percent increase from TF200 to TF1000
NaCl (180,000 ppm)	39.6 %	56.9 %
$MgCl_2$ (95,210 ppm)	15.0 %	26.36 %

Na_2SO_4 (142,040 ppm)	10.9 %	23.22 %
Na_2CO_3 (21,197 ppm)	21.7 %	25.0 %

With regard to the rejection factor, Figures 7-10 reveal the relation between the concentration, pore size and rejection. The rejection factor decreases with increasing concentration for TF1000. However, it rose slightly for TF450 and remains constant for TF200. Similar results have also been reported by Drioli et al. [7]. He et al. [32] and Calabro et al. [33] confirm that the decrease in rejection factor was due to the decrease in LEP (Liquid Entry Pressure) because liquid entry pressure (LEP) reduces when the pore size increases under higher concentration conditions. In addition, Khayet and Matsuura [34] proposed that, the surface membrane pore size is different from bulk pore size, and pore size is not cylindrical as assumed. Furthermore, liquid entry pressure (LEP) reduces when the pore size increases. Besides that, the possibility of membrane fouling increases with increasing salt concentration. Scale formation and deposition at membrane surfaces may reduce the membrane hydrophobicity; so the saline solution will go through some membrane pores [21]. Moreover, fouling and scaling lead to block the membrane pores, which reduce the permeate flux and may cause a pressure drop too [17]. Gryta et al. [35] reported that the scale formation and deposition on the membrane surface starts in the largest pores . For these reasons, TF450 and TF1000 membranes were wetted at 42,000 ppm Na_2CO_3, as is shown in figure 9. Consequently, using TF450 and TF1000 membranes is not recommended to treat 42,000 ppm Na_2CO_3 and higher.

4.4 Energy Consumption

The energy consumption considered in this work referred only to the amount of electric energy consumed (in kWh) for external heat supply, the cooling systems and for the pump used for re-circulating feed. The effect of salt concentration on the energy consumption was explored using TF200, TF450 and TF1000 membranes. Figures 11-14 illustrate that as the salt concentration of NaCl, $MgCl_2$, Na_2SO_4 and Na_2CO_3 increases, the energy consumption ratio increases. For TF200, for example, the energy consumption /permeate flux production ratio was 0.016, 0.023, 0.028 and 0.034 kWh/g for NaCl concentrations of 5,844; 35,064; 116,880 and 180,000 ppm respectively. The rise in energy consumption as the concentration increases can be explained by the fact that the higher the concentration, the higher the boiling point. It is worth noting that the viscosity and water activity are function of feed concentration. Because of the high concentration, the flow and water vapour pressure will be affected negatively. Therefore, it was predicted that feed concentration had a negative impact on the energy consumption for the process [36, 37]. Similar results have also been reported elsewhere; Sharqawy et al. [12] specified that increasing the salinity led to higher boiling temperature.

It was noted from the experiments that the energy consumption as kWh was almost equal even though pore size increased. However, energy consumption as kWh / permeate flux production ratio was found to be slightly lower as pore size increased, because of the positive effect of pore size on flux when it increases.

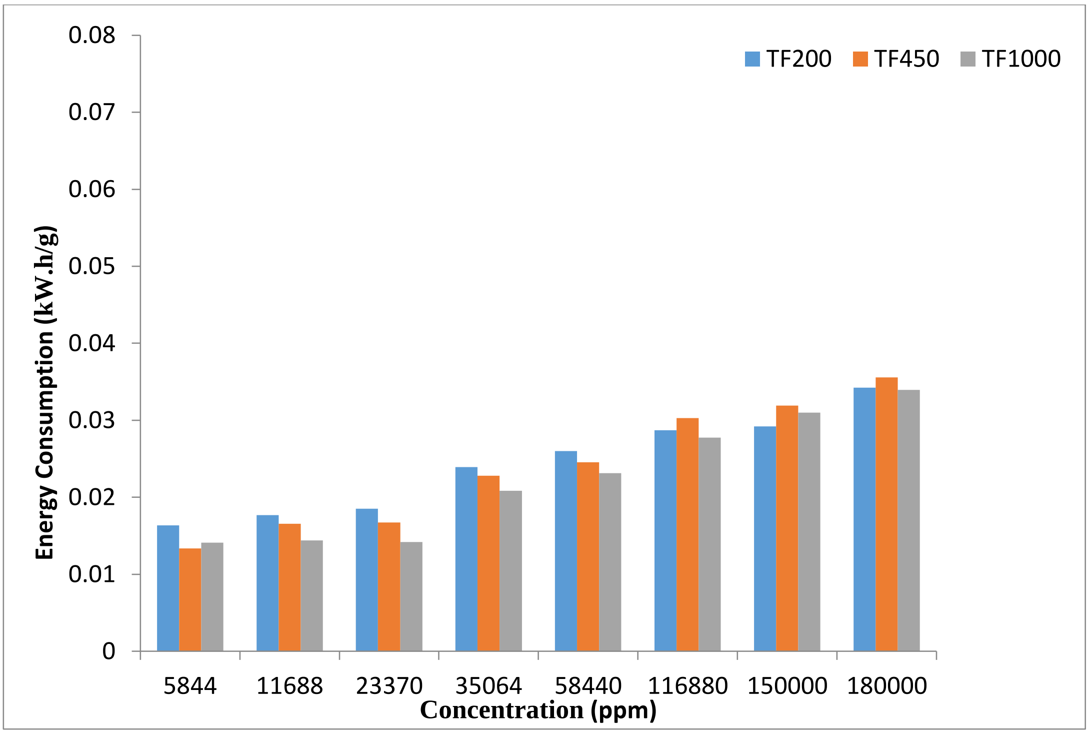

Fig. 11. Energy consumption for NaCl at different concentrations

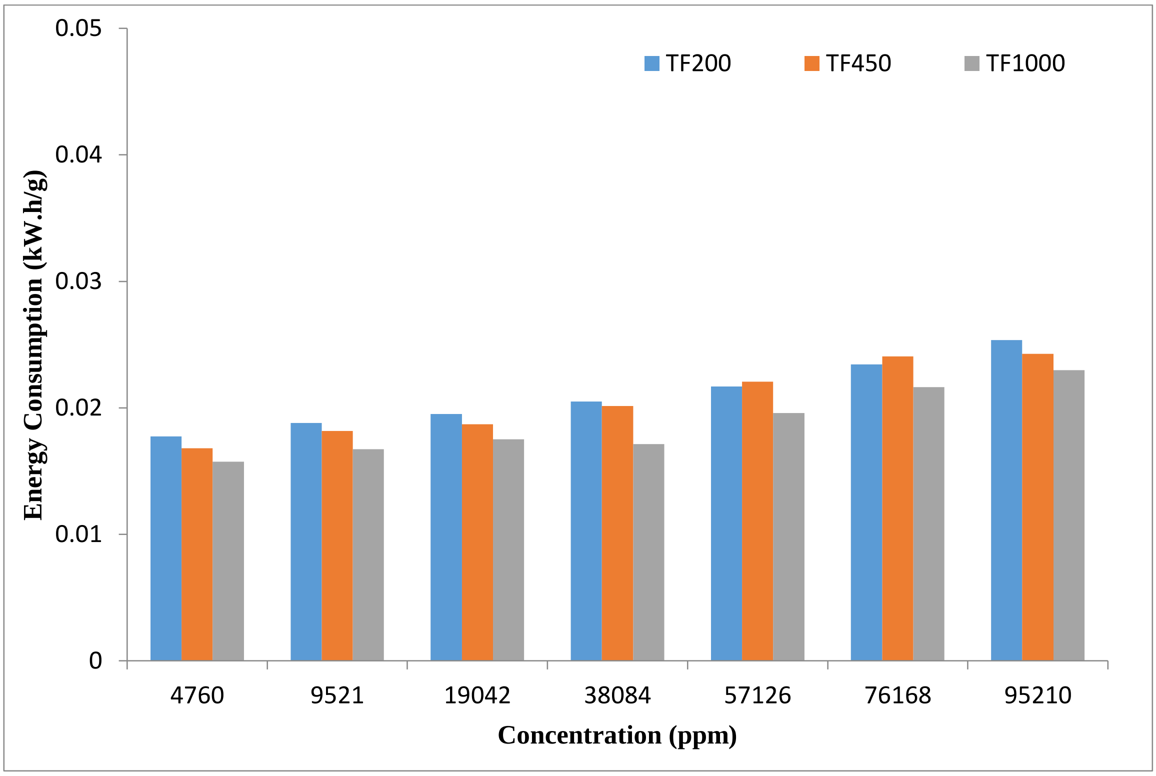

Fig. 12. Energy consumption for $MgCl_2$ at different concentrations

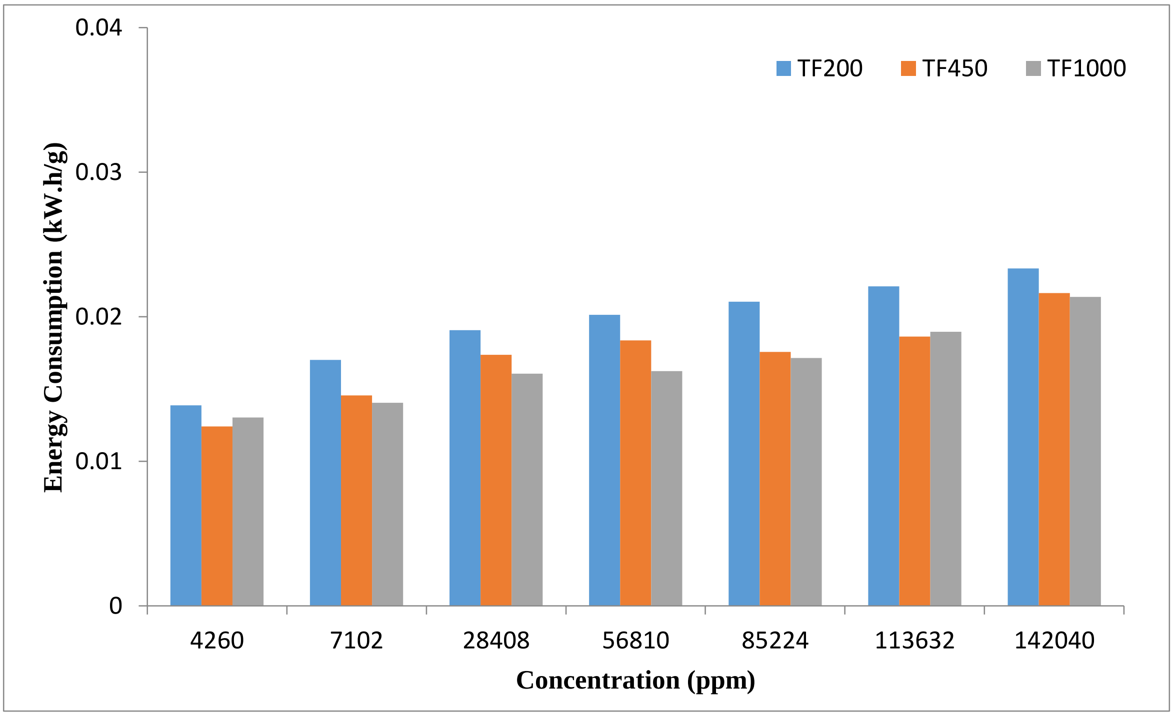

Fig. 13. Energy consumption for Na_2SO_4 at different concentrations

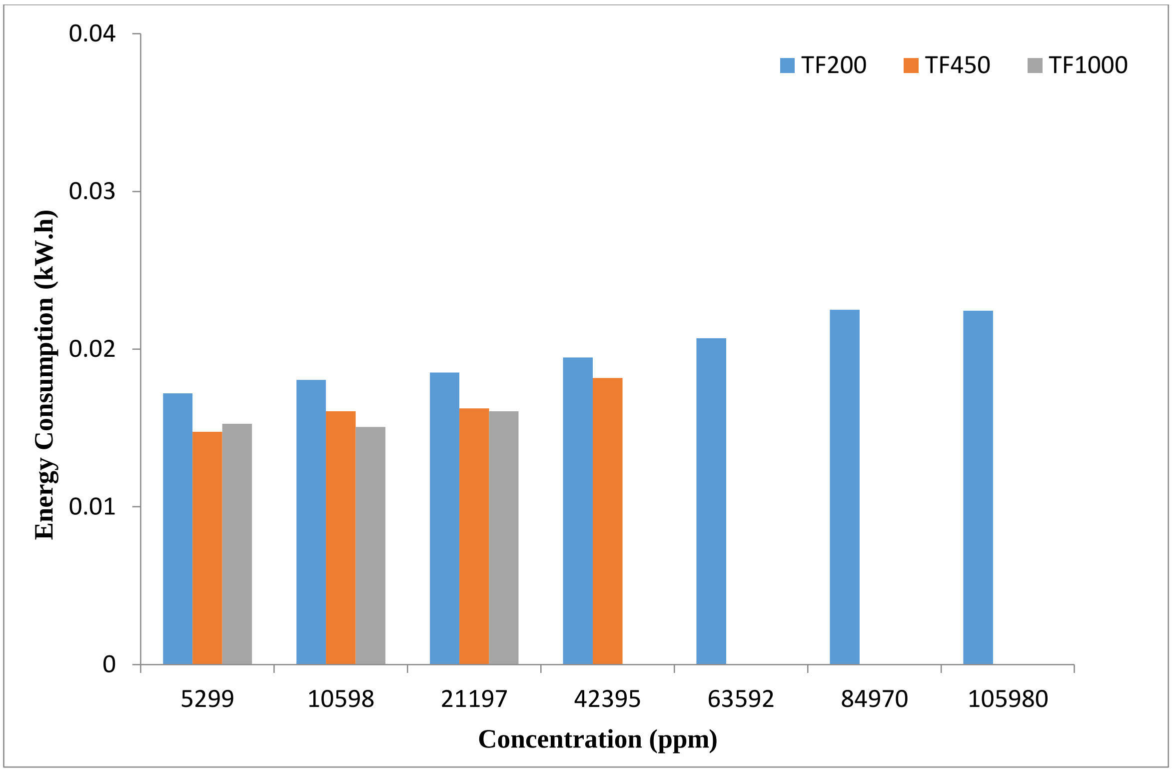

Fig. 14. Energy consumption for Na_2CO_3 at different concentrations

4.5 Conclusion

An experimental study using four different salts (NaCl, $MgCl_2$, Na_2CO_3, and Na_2SO_4) and three microporous membranes (TF200, TF450 and TF1000) was performed using AGMD. A wide range of concentrations for the previous salts was studied. The effect of high salt concentration was tested. In particular, the influence of salt concentration on permeate flux, rejection factor and energy consumption for different membrane pore sizes was examined. The major findings can be summarised as follows:

- The vapour pressure plays a noticeable role in permeate flux. For instance, the permeate flux declines when salt solution increases.
- The permeate flux decline is higher than that predicted from the vapour pressure reduction. The explanation of this decrease is attributed to the fouling phenomenon,

change in the solution layer features on the membrane surface, such as viscosity, and the temperature polarization.

- The permeate flux raises, as expected, When the pore size increases due to the enhanced mass transfer in the pores.
- The rejection factor decreases with the increasing salt concentration for TF1000. However, it declined slightly for TF450 and remained constant for TF200. This can be attributed to the decrease in LEP (Liquid Entry Pressure) under higher concentration conditions.
- TF200 membrane revealed a great hydrophobicity compared to TF450 and TF1000 for Na_2CO_3.
- The energy consumption increased when the concentration increased. This can be explained by the fact that the higher the concentration, the higher the boiling point.
- Energy consumption as kW.h per g production was found to slightly decline with pore size increase, because of the positive effect of pore size on flux, which increases.

References

1. Alkhudhiri, A., N. Darwish, and N. Hilal, *Treatment of high salinity solutions: Application of air gap membrane distillation.* Desalination, 2012. **287**(0): p. 55-60.
2. Alkhudhiri, A., N. Darwish, and N. Hilal, *Membrane distillation: A comprehensive review.* Desalination, 2012. **287**(0): p. 2-18.
3. Banat, F.A. and J. Simandl, *Theoretical and experimental study in membrane distillation.* Desalination, 1994. **95**(1): p. 39-52.
4. Bandini, S. and G.C. Sarti, *Heat and mass transport resistances in vacuum membrane distillation per drop.* 1999. **45**: p. 1422-1433.
5. Bandini, S., C. Gostoli, and G.C. Sarti, *Separation efficiency in vacuum membrane distillation.* Journal of Membrane Science, 1992. **73**(2-3): p. 217-229.
6. Kurokawa, H., O. Kuroda, S. Takahashi, and K. Ebara, *Vapor Permeate Characteristics of Membrane Distillation.* Separation Science and Technology, 1990. **25**(13): p. 1349 - 1359.
7. drioli, E., V. Calabro, and Y. Wu, *Microporous membranes in membrane distillation.* Pure & Appl. Chem, 1986. **58**(12): p. 1657-1662.
8. Martínez, L., *Comparison of membrane distillation performance using different feeds.* Desalination, 2004. **168**: p. 359-365.
9. Safavi, M. and T. Mohammadi, *High-salinity water desalination using VMD.* Chemical Engineering Journal, 2009. **149**(1-3): p. 191-195.
10. Yun, Y., R. Ma, and A.G. Fane, *Direct contact membrane distillation mechanism for high concentration NaCl solutions.* Desalination, 2006. **188**(1-3): p. 251-262.

11. Alkhudhiri, A., N. Darwish, and N. Hilal, *Produced water treatment: Application of Air Gap Membrane Distillation.* Desalination, 2013. **309**(0): p. 46-51.
12. Sharqawy, M.H., J.H. Lienhard, and S.M. Zubair, *Thermophysical properties of seawater: a review of existing correlations and data.* Desalination and Water Treatment, 2010. **16**(1-3): p. 354-380.
13. Ge, X. and X. Wang, *Estimation of Freezing Point Depression, Boiling Point Elevation, and Vaporization Enthalpies of Electrolyte Solutions.* Industrial & Engineering Chemistry Research, 2009. **48**(4): p. 2229-2235.
14. Hunter, J.B. and H. Bliss, *Thermodynamic Properties of Aqueous Salt Solutions.* Industrial & Engineering Chemistry, 1944. **36**(10): p. 945-953.
15. Weissenborn, P.K. and R.J. Pugh, *Surface Tension of Aqueous Solutions of Electrolytes: Relationship with Ion Hydration, Oxygen Solubility, and Bubble Coalescence.* Journal of Colloid and Interface Science, 1996. **184**(2): p. 550-563.
16. Li, J., Y. Guan, F. Cheng, and Y. Liu, *Treatment of high salinity brines by direct contact membrane distillation: Effect of membrane characteristics and salinity.* Chemosphere, 2015. **140**: p. 143-149.
17. Kullab, A. and A. Martin, *Membrane distillation and applications for water purification in thermal cogeneration plants.* Separation and Purification Technology, 2011. **76**(3): p. 231-237.
18. Gryta, M., *Long-term performance of membrane distillation process.* Journal of Membrane Science, 2005. **265**(1-2): p. 153-159.
19. Gryta, M., *Fouling in direct contact membrane distillation process.* Journal of Membrane Science, 2008. **325**(1): p. 383-394.
20. Goh, S., J. Zhang, Y. Liu, and A.G. Fane, *Fouling and wetting in membrane distillation (MD) and MD-bioreactor (MDBR) for wastewater reclamation.* Desalination, 2013. **323**: p. 39-47.
21. El-Bourawi, M.S., Z. Ding, R. Ma, and M. Khayet, *A framework for better understanding membrane distillation separation process.* Journal of Membrane Science, 2006. **285**(1-2): p. 4-29.
22. Tun, C.M., A.G. Fane, J.T. Matheickal, and R. Sheikholeslami, *Membrane distillation crystallization of concentrated salts--flux and crystal formation.* Journal of Membrane Science, 2005. **257**(1-2): p. 144-155.
23. Meltzer, T.H. and M.W. Jornitz, *Filtration and Purification in the Biopharmaceutical Industry, Second Edition*. 2008: Taylor & Francis Group.
24. Miyawaki, O., A. Saito, T. Matsuo, and K. Nakamura, *Activity and Activity Coefficient of Water in Aqueous Solutions and Their Relationships with Solution Structure Parameters.* Bioscience, Biotechnology, and Biochemistry, 1997. **61**(3): p. 466-469.
25. Guendouzi, M.E. and A. Dinane, *Determination of water activities, osmotic and activity coefficients in aqueous solutions using the hygrometric method.* The Journal of Chemical Thermodynamics, 2000. **32**(3): p. 297-310.
26. Sparrow, B.S., *Empirical equations for the thermodynamic properties of aqueous sodium chloride.* Desalination, 2003. **159**(2): p. 161-170.
27. Poling, B.E., G.H. Thomson, D.G. Friend, R.L. Rowley, and W.V. Wildind, eds. *Physical and Chemeical Data*. Perry's Chemical Engineering Handbook, ed. R.H. Parry and D.W. Green. 1997, McGraw-Hill.
28. Qtaishat, M., T. Matsuura, B. Kruczek, and M. Khayet, *Heat and mass transfer analysis in direct contact membrane distillation.* Desalination, 2008. **219**(1-3): p. 272-292.
29. Lawson, K.W. and D.R. Lloyd, *Membrane distillation.* Journal of Membrane Science, 1997. **124**(1): p. 1-25.
30. Alkhudhiri, A., N. Darwish, and N. Hilal, *Treatment of saline solutions using Air Gap Membrane Distillation: Experimental study.* Desalination, 2013. **323**(0): p. 2-7.
31. Shirazi, S., C.-J. Lin, and D. Chen, *Inorganic fouling of pressure-driven membrane processes -- A critical review.* Desalination, 2010. **250**(1): p. 236-248.

32. He, K., H. Hwang, and I. Moon, *Air gap membrane distillation on the different types of membrane.* Korean Journal of Chemical Engineering, 2011. **28**(3): p. 770-777.
33. Calabro, V., G. Pantano, M. Kang, R. Molinari, and E. Drioli, *Experimental study on integrated membrane processes in the treatment of solutions simulating textile effluents. Energy and exergy analysis.* Desalination, 1990. **78**(2): p. 257-277.
34. Khayet, M. and T. Matsuura, *Determination of surface and bulk pore sizes of flat-sheet and hollow-fiber membranes by atomic force microscopy, gas permeation and solute transport methods.* Desalination, 2003. **158**(1â€“3): p. 57-64.
35. Gryta, M., M. Tomaszewska, and K. Karakulski, *Wastewater treatment by membrane distillation.* Desalination, 2006. **198**(1–3): p. 67-73.
36. Bui, V.A., M.H. Nguyen, and J. Muller, *The energy challenge of direct contact membrane distillation in low temperature concentration.* Asia-Pacific Journal of Chemical Engineering, 2007. **2**(5): p. 400-406.
37. Al-Obaidani, S., E. Curcio, F. Macedonio, G. Di Profio, H. Al-Hinai, and E. Drioli, *Potential of membrane distillation in seawater desalination: Thermal efficiency, sensitivity study and cost estimation.* Journal of Membrane Science, 2008. **323**(1): p. 85-98.